

SP-ViT: Learning 2D Spatial Priors for Vision Transformers

Yuxuan Zhou^{1*}, Wangmeng Xiang^{2*}, Chao Li⁴, Biao Wang⁴, Xihan Wei⁴
 Lei Zhang², Margret Keuper³, Xiansheng Hua⁴

zhouyuxuanyx@gmail.com

¹ University of Mannheim

² The Hong Kong Polytechnic University

³ University of Siegen, Max Planck Institute for Informatics, Saarland Informatics Campus

⁴ Alibaba Group

ABSTRACT

Recently, transformers have shown great potential in image classification and established state-of-the-art results on the ImageNet benchmark. However, compared to CNNs, transformers converge slowly and are prone to overfitting in low-data regimes due to the lack of spatial inductive biases. Such spatial inductive biases can be especially beneficial since the 2D structure of an input image is not well preserved in transformers. In this work, we present Spatial Prior-enhanced Self-Attention (SP-SA), a novel variant of vanilla Self-Attention (SA) tailored for vision transformers. Spatial Priors (SPs) are our proposed family of inductive biases that highlight certain groups of spatial relations. Unlike convolutional inductive biases, which are forced to focus exclusively on hard-coded local regions, our proposed SPs are learned by the model itself and take a variety of spatial relations into account. Specifically, the attention score is calculated with emphasis on certain kinds of spatial relations at each head, and such learned spatial foci can be complementary to each other. Based on SP-SA we propose the SP-ViT family, which consistently outperforms other ViT models with similar GFlops or parameters. Our largest model SP-ViT-L achieves a record-breaking 86.3% Top-1 accuracy with a reduction in the number of parameters by almost 50% compared to previous state-of-the-art model (150M for SP-ViT-L \uparrow 384 vs 271M for CaiT-M-36 \uparrow 384) among all ImageNet-1K models trained on 224×224 and fine-tuned on 384×384 resolution w/o extra data.

1 INTRODUCTION

Transformers [22] have recently achieved exciting results in image classification [3–5, 7, 8, 11, 13, 15, 20, 21, 24, 26, 27, 29], after dominating in natural language processing (NLP) tasks [1, 6, 14]. At the heart of all transformers lies the so-called self-attention mechanism, which captures the content relations between all pairs of input tokens globally and focuses on related pairs selectively. Self-attention is more flexible in comparison to convolution, which is hard-coded to capture local dependencies exclusively. This can possibly equip transformer models with larger capacity and greater potential for computer vision tasks. As reported in recent works, transformers outperform Convolutional Neural Networks (CNNs), when pretrained on large dataset [8], facilitated with knowledge distillation [20] or pseudo labels [13] from pretrained CNNs.

Nevertheless, CNNs generalize better and converge faster than Vision Transformers (ViT). This suggests that certain types of inductive biases employed in convolution can still be beneficial to

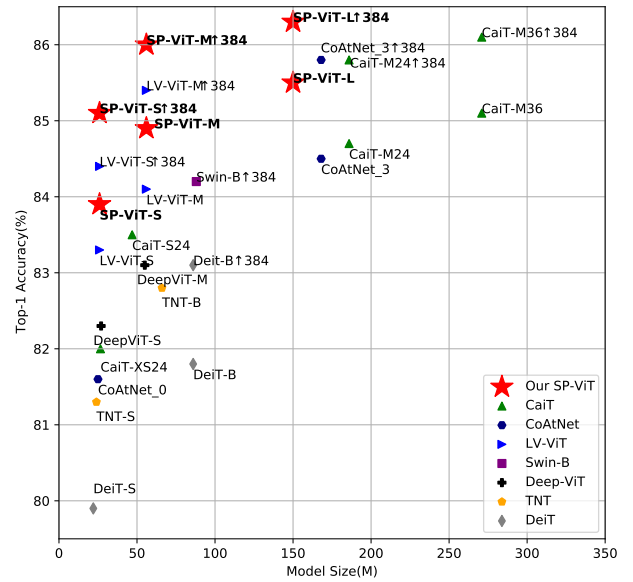


Figure 1: ImageNet-1K top-1 accuracy of our proposed SP-ViT and state-of-the-art ViTs. The models shown are all trained on 224×224 resolution, \uparrow denotes that models are fine-tuned on a higher resolution. Note that we exclude models pretrained on extra data or larger resolution than 224×224 for a fair comparison.

solving vision tasks. Not surprisingly, many recent studies [4, 5, 7, 10, 15, 20, 24, 26, 27] propose to incorporate convolutional inductive biases into ViTs in different ways and all demonstrate boosted performance. The effectiveness of convolution relies on the fact that neighboring pixels of natural images are highly correlated, but there may exist other highly correlated contents outside the local receptive field of a convolutional filter that are ignored. Therefore, we propose to make use of a variety of inductive biases simultaneously, just as humans do in our daily life, e.g., if we see a part of a horizontal object, we naturally look along its direction instead of restricting our sight within a local area.

*Work done as Intern at Alibaba Group

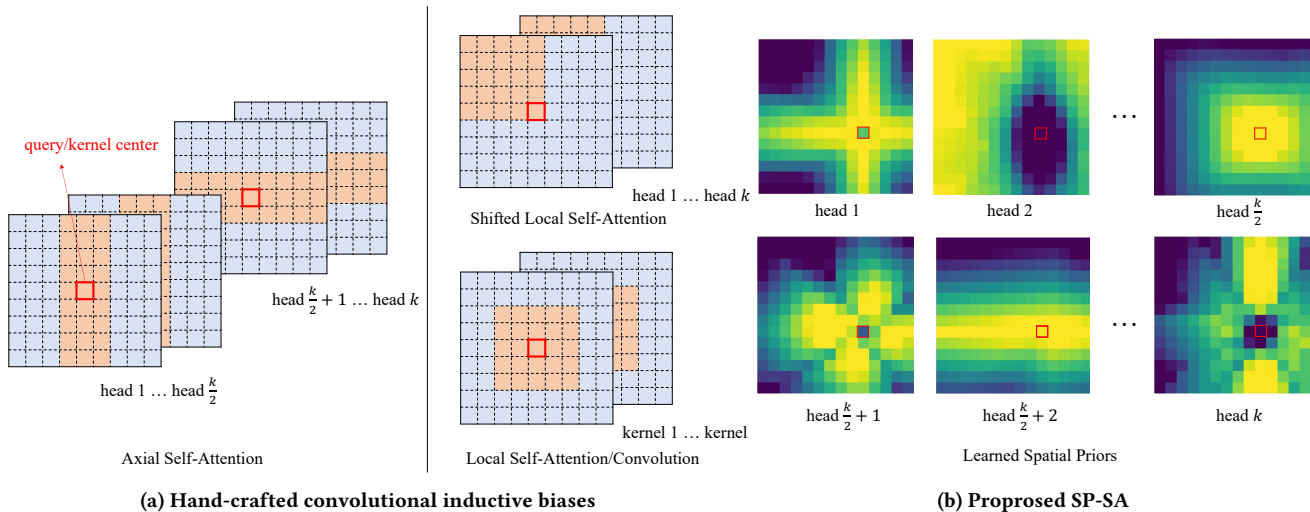


Figure 2: (a) Examples of convolutional inductive biases proposed for ViTs: axial self-attention in CSWin-Transformer [7] and shifted local self-attention in Swin-Transformer [15]. (b) The presented Spatial Priors (SPs) are learned by our model automatically. The learned SPs assign different scores for different spatial relations. Given a certain SP, attention is forced to be within high-score regions. It can be seen that our SP-SA handles different types of spatial relations in a complementary manner, e.g., SPs which focus on local and non-local relations are both learned by our model. Consequently, a more global receptive field can be maintained at a single layer.

In this work, we introduce a novel family of inductive biases named *Spatial Priors* (SPs) into ViTs via an extension of vanilla self-attention (SA), called *Spatial Prior-enhanced Self-Attention* (SP-SA). SP-SA highlights a certain group of 2D spatial relations at each attention head based on the relative position of the key and query patches. It facilitates the calculation of attention scores within the context of such types of spatial relations. Since the construction and validation of appropriate spatial priors are extremely laborious, we introduce the idea of *learnable spatial priors*. More specifically, we only impose the weak prior knowledge to the model that different relative distances should be treated differently. Yet we do not force the model to favor any kind of spatial relation in advance, e.g., neither local nor non-local. Effective spatial priors (SPs) are supposed to be discovered by the model itself in the training stage. For this purpose, SPs are represented by a family of mathematical functions which map the relative coordinates to abstracted scores, called *spatial relation functions*. To search for desirable spatial relation functions, we parameterize these functions by neural networks and optimize them jointly with ViTs. Thereby, the model can learn spatial priors similar to the ones induced in convolutions, but it can also learn spatial relationships over larger distances.

Examples for learned SPs are shown in Fig. 2(b). Diverse complementary patterns are presented in different attention heads, so that different types of spatial relations are handled individually. At the same time, a global receptive field is approximately composed by considering all heads together.

As a matter of fact, convolutional inductive biases can be seen as a special kind of spatial priors: they first divide coordinate spatial relations into two categories, i.e., ones focusing on the local neighborhood and ones focusing on non-local regions. Then they learn priors of the local neighborhoods and ignore the non-local relations.

For comparison, some of the existing approaches to combine such convolutional biases with ViTs are illustrated in Fig. 2(a). Based on a local window, new variants are proposed for CSWin-Transformer [7] and Swin-Transformer [15] by changing the aspect ratio or shifting the center respectively. However, the design of such windows is extremely intuitive and the main idea of focusing on local relations remains unchanged.

In summary, we make the following contributions:

- We propose a family of inductive biases for ViTs that focus on different types of spatial relations, called Spatial Priors (SP). SPs generalize the locally restricted convolutional inductive biases to both local and non-local correlations. Parameterized with neural networks, SPs are automatically learned during training, without imposing a preference for any hard-coded region in advance.
- We propose SP-SA, a novel self-attention variant that automatically learns beneficial 2D spatial inductive biases. Built on our proposed SP-SA, we further construct a ViT variant called SP-ViT. SP-ViTs achieve state-of-the-art results on the ImageNet Benchmark w/o extra data, e.g., SP-ViT-L \uparrow 384 yields a record-breaking 86.3% Top-1 accuracy with only around half the amount of parameters of the previous best-performing model CaiT-M-36 \uparrow 384.
- Our proposed SPs are compatible with various input sizes, as they are derived from relative coordinates between each pair of patches instead of their absolute positions. SP-ViTs also demonstrate improved performance over the baseline model on Image Classification when fine-tuned on higher resolution.

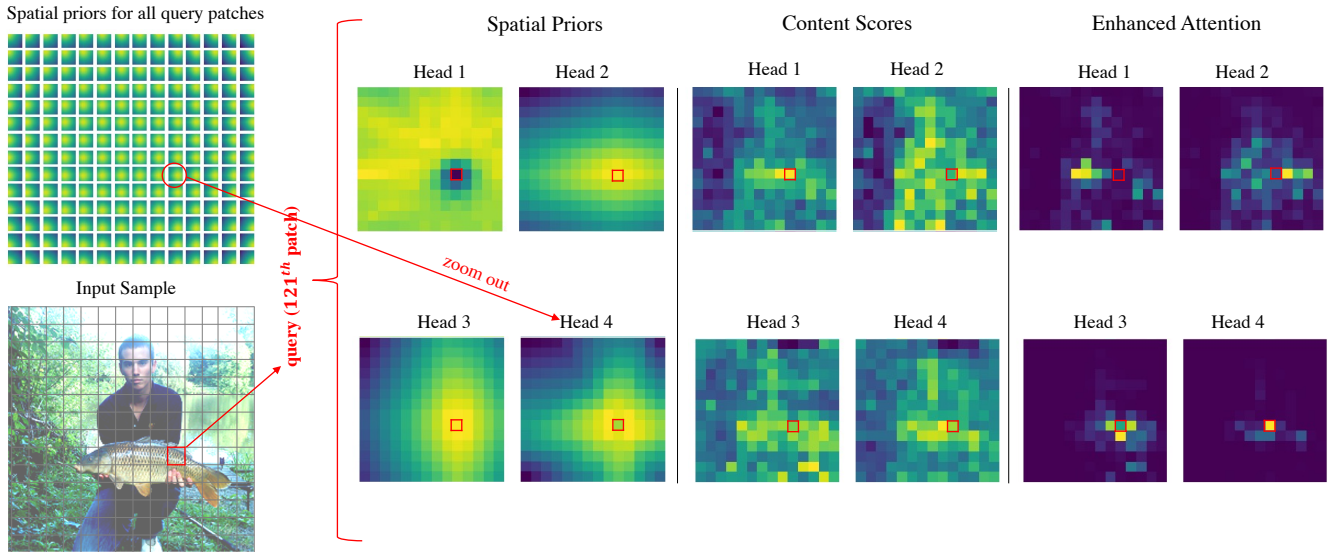


Figure 3: Visualization of the learned 2D SPs, content scores and the enhanced attention at the first 4 heads of layer 4. The input image is shown in the bottom-left and the query patch is marked in red. Different SPs are learned, including horizontal and vertical (head 2 and 3), non-local (head 1), as well as cross-shaped (head 4). The attention scores at each head are obtained within the context of a certain type of spatial relations. The original attention is distracted by background objects, whereas our Spatial Priors help the model to focus on the object of interest.

2 RELATED WORK

2.1 Vision Transformers

Recently, Dosovitskiy et al. [8] showed that purely attention-based transformers can achieve state-of-the-art performance in image classification, when pre-trained on large-scale datasets. Since then, a vast amount of efforts have been made to improve ViTs. Some works [9, 13] find it effective to add additional losses or regularization terms, while others propose new patch embedding blocks [11] or scale-up methods [21, 29]. [7, 15, 23, 28] propose to utilize multi-scale information, where pyramid designs and local attention are often adopted to reduce the overall computation. It is noteworthy that an approximately cross-shaped 2D structure, which brings performance gain in CSWin-Transformer [7], is also learned automatically by our model.

2.2 Inductive Biases for Vision Transformers

The performance of ViTs degrades rapidly with a reduced amount of training data. To alleviate this issue, many studies focus on emphasizing local correlations by introducing a convolutional inductive bias into ViTs, either by restricting self-attention to local windows [7, 15], combining vanilla transformers with implicit or explicit convolutional operations [4, 10, 24, 26, 27], knowledge distillation [20], or convolutional initialization [5]. Our work also incorporates inductive biases into ViTs, but they are not locally restricted and automatically learned by the model. Indeed, as shown in Fig. 2(b), patterns that focus solely on local or remote regions are both present in the learned SPs.

2.3 Relative Spatial Information for ViTs

Transformers are by their very nature permutation invariant, thus extra spatial information is often supplied to make them more suitable for ordered input data. Besides the commonly adopted absolute positional embedding, the relative spatial information is also considered in Swin-Transformer [15] by an additional trainable bias term called relative positional bias. ConViT [5] also introduces a function taking coordinates relative to the query patch as input to force the attention to be within a local region. In comparison to ViTs, using relative positional information is more common in NLP transformers. The relative positional embedding [18] is built on the 1D distances between tokens and has been further improved in XL-Net [25] and DEBERTA [12]. However, the original relative positional embedding can be extended to 2D for ViTs with little effort. In contrast, our method not only provides 2D spatial information but also imposes learned priors about spatial relations on the model. The latter proves to be beneficial for learning a stronger model, see Sec. 4.2.

3 METHOD

3.1 Revisiting Multi-Head Self-Attention

Self-attention receives an input sequence $X = (\vec{x}_1, \dots, \vec{x}_n)$ and outputs a new sequence $Y = (\vec{y}_1, \dots, \vec{y}_n)$ of the same length, where each element is computed as weighted sum of the linearly transformed input elements:

$$\vec{y}_i = \sum_{j=1}^n A_{ij} (\vec{x}_j^T \mathbf{W}^V), \quad (1)$$

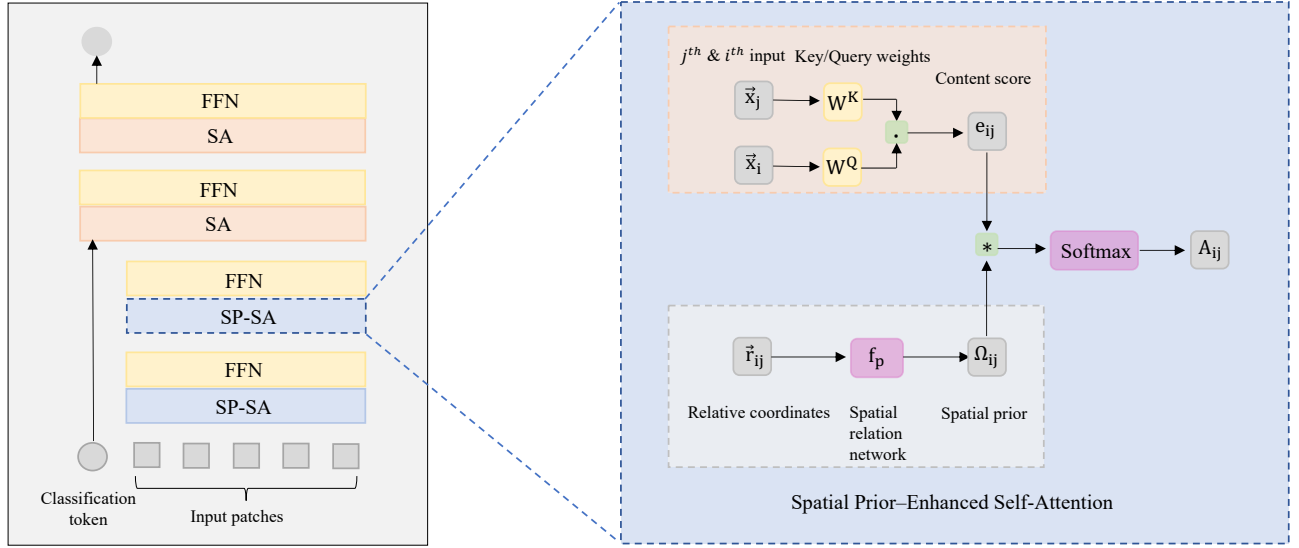


Figure 4: The schema of SP-ViT. SP-SA can be used as a drop-in replacement for the vanilla SA layer at a range of depths. Because the classification token does not have a valid 2D relative coordinate, it is simply concatenated with the hidden representation after the last SP-SA layer. FFN: feedforward network (2 linear layers separated by a GeLU activation).

each weight coefficient, or attention score A_{ij} , is determined based on the semantic dependencies between two elements, by applying a softmax function to the scaled dot product of linearly transformed elements e_{ij} , which we refer to as content score throughout this paper:

$$A_{ij} = \frac{\exp(e_{ij})}{\sum_{k=1}^n \exp(e_{ik})}, \quad (2)$$

with

$$e_{ij} = \frac{(\vec{x}_i^T \mathbf{W}^Q)(\vec{x}_j^T \mathbf{W}^K)^T}{\sqrt{d_z}}. \quad (3)$$

Multi-head self-attention employs several such operations in parallel to learn different kinds of interdependencies. The final output is obtained by applying a linear transformation to the concatenated outputs from each head.

3.2 Spatial Prior-enhanced Self-Attention

Motivated by the observation that certain types of inductive biases on spatial relations can be beneficial to transformers, we propose an extension of self-attention enhanced by a combination of learned 2D Spatial Priors (SPs), called Spatial Prior-enhanced Self-Attention (SP-SA).

Each SP $\Omega \in \mathbf{R}^{N \times N}$ forms a kind of spatial context for computing attention scores $\mathbf{A} \in \mathbf{R}^{N \times N}$, and it is derived from coordinate spatial relations between input element pairs, i.e. relative positions between the key and query patches for ViTs. Thus an SP has exactly the same form of attention scores and we can simply integrate it in Eq. (2) by multiplicative interaction:

$$A_{ij} = \frac{\exp(e_{ij} \cdot \Omega_{ij})}{\sum_{k=1}^n \exp(e_{ik} \cdot \Omega_{ik})}. \quad (4)$$

3.2.1 2D Spatial Prior. Taking query patch i as the reference point, we can obtain a relative coordinate $\vec{r}_{ij} \in \mathbf{R}^2$ for image patch j . Then we employ a shared mapping f_p for all query and key patch pairs, named spatial relation function:

$$\Omega_{ij} = f_p(\vec{r}_{ij}), \quad (5)$$

the outputs together form the so-called 2D SP Matrix Ω .

3.2.2 Learnable 2D Spatial Priors. To enable the model to learn desirable inductive biases automatically, we employ Multilayer Perceptron (MLP) to parameterize the mapping from 2D relative coordinates to Ω :

$$f_p(\vec{r}_{ij}) = \text{MLP}(\vec{r}_{ij}). \quad (6)$$

Thereby, we allow Ω to learn a weighting for the attention scores for query \vec{x}_i and key \vec{x}_j which depends solely on their relative coordinates and is applied in a non-linear way, i.e. before the softmax. We extend SP-SA to its multi-head version by adding a unique network to each head. This design follows the same motivation as multi-head self-attention and assumes that a combination of different SPs should boost the performance.

3.3 Relation to Other Methods

In the following, we discuss the similarities and differences of SP-SA to the most closely related works in detail.

3.3.1 Relation to Local Windows. The square and cross-shaped windows used in [7, 15] can be seen as a special form of our proposed spatial relation functions in practice:

$$f_p(\vec{r}_{ij}) = \begin{cases} 1, & \text{if } \|(\vec{r}_{ij} - \vec{\Delta}) \odot (a, b)\|^\infty \leq 1 \\ & \text{or } \|(\vec{r}_{ij} - \vec{\Delta}) \odot (b, a)\|^\infty \leq 1, \\ 0, & \text{else} \end{cases} \quad (7)$$

where $\bar{\Delta}$, a and b control the shift, window width and height respectively. If $a = b$, it generates a square window, otherwise it results in a cross-shaped window. Both works only adopt some hard-coded patterns for the whole network, while our method proposes to benefit from a variety of beneficial 2D structures.

3.3.2 Relation to PSA. The Positional Self-Attention (PSA) proposed by d’Ascoli et al. [5] can also be regarded as a manually designed family of spatial relation functions:

$$f_p(\vec{r}_{ij}) = \alpha(\|(\Delta_x, \Delta_y)\|^2 - \|\vec{r}_{ij} - (\Delta_x, \Delta_y)\|^2), \quad (8)$$

where Δ_x and Δ_y are learnable parameters, which are initialized following an explicit rule to approximate convolution effect.

Note that their main contribution is the so-called local/convolutional initialization, which restricts the number of heads to the square of integer numbers, and the initial values of both α and $\bar{\Delta}$ require extra hyperparameter tuning. In order to compare with their method, we adopt a ViT baseline with 9 heads for our ablation analysis as in [5]. Moreover, it may be possible to extend their proposed local initialization to our SP-SA, leveraging the merits of both methods. We leave this to future work.

3.3.3 Relation to Relative Positional Embeddings. Shaw et al. [18] introduce the so-called 1D relative positional embedding for transformers to take relative distances into account:

$$A_{ij} = \frac{\exp(e_{ij} + (\vec{x}_i \mathbf{W}^Q) T_{r_{ij}})}{\sum_{k=1}^n \exp(e_{ik} + (\vec{x}_i \mathbf{W}^Q) T_{r_{ij}})}, \quad (9)$$

where T is a learnable embedding table from which the relative positional embedding is taken. Then it interacts multiplicatively with the query.

Unlike 1D relative positional embeddings, our proposed spatial relation functions have more power in modeling the 2D structures of images. If extended to 2D, their method is equivalent to applying a linear transformation to one-hot representations of relative distances. For one-hot representations, the magnitude of distances is neglected, while this is not the case for relative coordinates. More importantly, Shaw et al. [18] simply add relative positional embeddings to key and value in the attention equation. The modification of self-attention is rather intuitive but lacks a clear physical interpretation. As opposed to positional embeddings, our method not only provides neutral positional information but also learns and injects beneficial inductive biases into the model.

The proposed SP-SA offers more flexibility than the above discussed approaches. We also confirmed experimentally that our proposed SA variant outperforms these methods, see Tab. 4.

4 EXPERIMENTS

We first provide an experimental evaluation of the proposed SP-SA in the context of image classification on the ImageNet-1k dataset and show that SP-ViTs achieve state-of-the-art results for training without extra data. Further, we provide an extensive ablation study to analyze the impact of all proposed model details.

4.1 Image Classification on ImageNet-1K

4.1.1 Settings. All models for ImageNet-1K classification are trained on a single machine node with 8 Tesla V100 GPUs. Our code is based on PyTorch [17] and the official implementation of DeiT [20]. To

Table 1: Comparing to state-of-the-art models trained on ImageNet-1k 224 × 224 resolution. Models are by default trained and tested on 224 × 224 resolution if not specified. ↑ plus size denotes the model is trained on 224 × 224 resolution then fine-tuned and tested on size × size resolution. The performance of LV-ViT-L trained on 224 × 224 resolution is not available in [13]. And LV-ViT-L trained on 288 × 288 resolution has a lower accuracy of 85.3%.

Network	Top-1 (%)	Parameters	FLOPs
DeiT-S [20]	79.9	22M	4.6B
DeepViT-S [29]	82.3	27M	6.2B
T2T-ViT-14 [27]	81.5	22M	5.2B
TNT-S [11]	81.3	24M	5.2B
CaiT-XS-24 [21]	82.0	27M	5.4B
LV-ViT-S [13]	83.3	26M	6.6B
EfficientNet-B5 [19]	83.6	30M	9.9B
Our SP-ViT-S	83.9	26M	6.6B
DeiT-B [20]	81.8	86M	17.5B
T2T-ViT-24 [27]	82.3	64M	14.1B
ConViT-B [5]	82.4	86M	17.5B
TNT-B [27]	82.8	66M	14.1B
Swin-S [15]	83.0	50M	8.7B
DeepViT-L [29]	83.1	55M	12.5B
Swin-B [15]	83.3	88M	15.4B
CaiT-S-24 [21]	83.5	47M	9.4B
ConvNeXt-B [16]	83.8	89M	15.4B
EfficientNet-B5 [19]	84.0	43M	19.0B
LV-ViT-M [13]	84.1	56M	12.7B
Our SP-ViT-M	84.9	56M	12.7B
ConvNeXt-L [16]	84.3	198M	34.4B
CoAtNet-3 [4]	84.5	168M	34.7B
CaiT-M-24 [21]	84.7	186M	36.0B
Our SP-ViT-L	85.5	150M	34.7B
T2T-ViT-14↑384 [27]	83.3	22M	17.1B
CoAtNet-0↑384 [4]	83.9	25M	13.4B
LV-ViT-S↑384 [13]	84.4	26M	22.2B
SP-ViT-S↑384	85.1	26M	22.2B
Swin-B↑384 [15]	84.2	88M	47.0B
CaiT-S-24↑384 [21]	85.1	47M	32.2B
LV-ViT-M↑384 [13]	85.4	56M	42.2B
Our SP-ViT-M↑384	86.0	56M	42.2B
CoAtNet-3↑384 [4]	85.8	168M	107.4B
CaiT-M-24↑384 [21]	85.8	186M	116.1B
CaiT-M-36↑384 [21]	86.1	271M	173.3B
Our SP-ViT-L↑384	86.3	150M	110.6B

obtain our SP-ViT model, we replace the vanilla SA layers of the DeiT baseline with our proposed SP-SA till the last 2 layers and follow the default training settings in [13] (data augmentations, training schedule, hyperparameters such as batch size, total number of layers etc.). We keep the vanilla SA in the last 2 layers, based

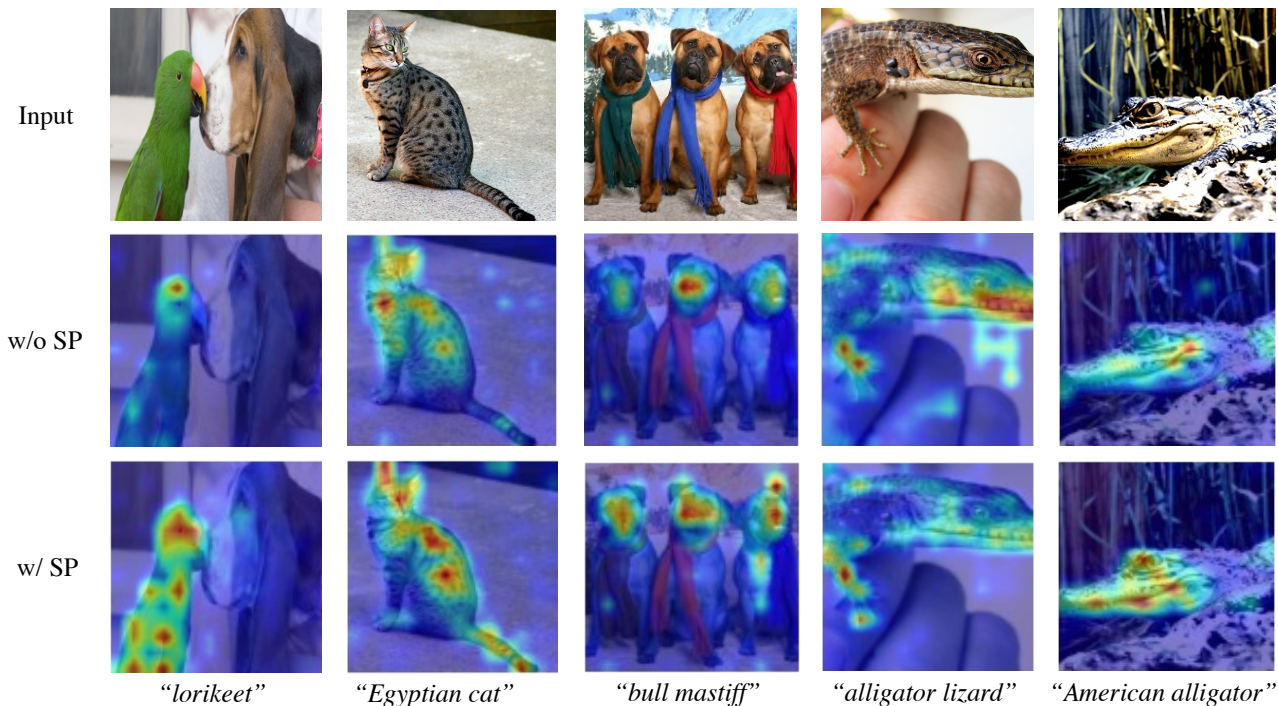


Figure 5: Visualization using Transformer Explainability [2]. The second row are results of DeiT baseline, which has no SP layers. The Last row are results of SP-ViT. Our SP-ViT generate results which have more focus on areas of interests and less distraction from background comparing to DeiT.

on the preliminary ablation analysis conducted on a fraction of ImageNet. Please refer to Sec. 4.2 for more details. When fine-tuning on 384×384 resolution (indicated by $\uparrow 384$ in Tab. 1), we set the batch size to 512, the learning rate to $5e-6$, the weight decay to $1e-8$ and we fine-tune the model for 30 epochs. For more details please refer to the Appendix.

4.1.2 Comparing to State-of-the-Art Models. We compare our proposed SP-ViT (taking LV-ViT as our baseline) with other recent ViTs in Tab. 1, including DeiT [20], TNT [11], T2T [27], Swin Transformer [15], DeepViT [29], LV-ViT [13], Swin Transformer [15], CaiT [21], etc.. The models in Tab. 1 are grouped according to comparable model sizes in terms of their number of parameters. Within all groups, the proposed SP-ViT outperforms competing models in terms of Top-1 accuracy. Our best result with Top-1 accuracy of 86.3% is achieved with the SP-ViT-L $\uparrow 384$ model. It outperforms all previous models while only having about 150M parameters as compared to 271M parameters of the second best model CaiT-M-36 $\uparrow 384$. Also note that our smaller model SP-ViT-M $\uparrow 384$ already achieves a Top-1 accuracy of 86.0% which is on par with CaiT-M-36 $\uparrow 384$ while reducing the amount of parameters from 271M to 56M (i.e. by a factor of about 4.8).

In the following, we first analyze our results in terms of class activation visualizations and then show ablation studies on our model components.

4.1.3 Qualitative results. We present visualizations of target class activation maps using the recent Transformer Explainability [2]

for several images in Figure 5 to showcase the behavior of SP-ViT. While the DeiT model only shows class activations on small parts of the target class regions, for example on the head of the “Lorikeet”, the fur of the “Egyptian cat” or the jaw of the “American alligator”, the proposed SP-ViT model shows class activations on wider target class regions. Thereby, it follows well class specific image regions such as the pointy ears as well as the tail of the “Egyptian cat”, and the dogs’ ears in the “Bull mastiff” class. The “Alligator lizard” example as well as the “American alligator” further show a significantly diminished class activation in background regions compared to DeiT. In summary, we make two observations: 1) The results that are generated by SP-ViT focus more on areas of target class objects comparing to DeiT. In “Lorikeet”, “Bull mastiff”, “Egyptian cat” and “American alligator”, SP-ViT’s activation maps clearly have a better coverage of target class; 2) The distraction by background is better suppressed, e.g. in “Alligator lizard”, which leads to a cleaner activation map.

4.2 Ablation Analysis

4.2.1 Settings. For the ablation study, we employ a small DeiT model as the baseline with 12 layers, 9 heads and 432 total number of embedded dimensions. The choice of the number of heads is simply for a fair comparison with other related methods, because Positional Self-Attention (PSA) introduced by d’Ascoli et al. [5] requires such specific numbers (square of integer numbers) of heads. Due to limited available computation resources, we train all model variants on the first 100 classes of ImageNet-1K called ImageNet-100

for 300 epochs, following the setup in [5]. In this section, we simply take the accuracy at the last epoch for all models. This should be a fair comparison, since we adopt the same hyperparameters for different models without tuning. For all experiments in this section, we train the models on 4 NVIDIA P100 GPUs and adopt a batch size of 256. The rest of settings are kept the same as DeiT’s w/o knowledge distillation in [20].

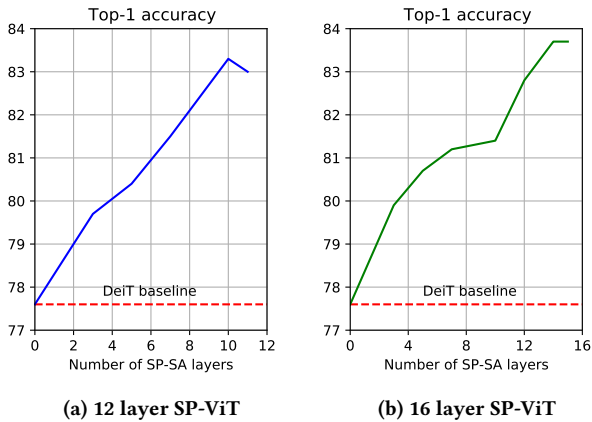


Figure 6: Top-1 accuracy(%) of SP-ViT on ImageNet-100 with different numbers of SP-SA layers. Fig. 6a and Fig. 6b show consistent improvements of our SP-ViT over DeiT Baselines with a total number of 12 and 16 layers respectively.

Table 2: Eliminate the effect of inserting the classification token at later layers on ImageNet-100.

Sub. layers	Cls token insertion layers	Top-1 (%)
0	0	77.6
0	10	81.7
10	10	83.3
0	Global Average Pooling	79.5
12	Global Average Pooling	81.7

4.2.2 *Numbers of Substituted SA Layers.* We first investigate how the performance of the SP-ViT is affected by the number of SP-SA layers. The layers are substituted from bottom to top of the model and a classification token is inserted after the last SP-SA layer.

It is shown in Fig. 6a that substituting a number of SA layers with SP-SA results in improved Top-1 accuracy comparing to DeiT baseline (0 layer). In general, the performance improves as more layers are substituted. For a model with 12 layers in total, the best performance is achieved when 10 layers are substituted. When substituting all but the last SA layer with our SP-SA, the performance drops slightly. We hypothesize that this is very likely because the classification token is only involved in the last layer, thus the class-specific features are not adequately extracted in such a case. We further investigated models with more layers in Fig. 6b (16 layers in

total), and found the similar trend. The best performance is achieved when the first to the penultimate layer are substituted.

As we have discussed in the section 3, we add the classification token directly after SP-SA layers because there is no valid 2D relative coordinate for it. In addition, to exclude the influence of inserting the classification token at deeper layers instead of the first, we conduct a further comparison in Tab. 2. It can be seen that the late insertion of the classification token does have a positive effect on the classification result, which is also observed by Touvron et al. [21]. However, as aforementioned, inserting the classification token after SP-SA layers is a natural design choice for our SP-ViT and the substitution of SP-ViT also increases the accuracy further.

Table 3: The effect of different hidden dimensions for our 2-layer MLP spatial relation function. Best results can be achieved with hidden dimension 32.

Hidden Dimension	Top-1 acc (%)
16	83.2
32	83.6
64	83.3
128	83.1

Table 4: Comparing to Self-Attention with Relative Positional Bias [15], Positional Self-Attention[5], Self-Attention with 1D Relative Positional Embedding (RPE) [18] and with its 2D extension as well as the 2D extension of a more advanced version of RPE proposed in DEBERTA [12] on ImageNet-100.

Method	Top-1 acc (%)
1D RPE [18]	80.1
2D RPE [18]	79.9
Improved 2D RPE [12]	82.8
Relative Positional Bias [15]	81.3
Positional Self-Attention [5]	82.5
SP-SA Additive	83.5
SP-SA	83.6

4.2.3 *Hidden Dimension of the 2-Layer MLP for the Spatial Relation Function.* We found that a simple 2-layer MLP works well as our spatial relation function. In Tab. 3, we investigate the impact of its hidden dimension on the performance. As we can see, the performance improves from a hidden dimension of 16 to 32 by 0.4% in Top-1 accuracy, but a further increase in the hidden dimension does not further improve results. Results for a hidden dimension of 32 are the best.

4.2.4 *Comparing to Relative Positional Embedding.* SP-SA Additive is obtained by simply replacing the multiplication in Eq. (4) with a summation. This setting is inferior to the original SP-SA, see Tab. 4, but it is more comparable to other existing methods which also employ additive interaction between spatial information and content

Table 5: Comparing to extended methods of introducing relative spatial information on ImageNet-100: Local SA (7x7 window), Relative Positional Coefficient (RPC) (analogous to Relative Positional Bias [15]), and SP-SA Linear (using a linear spatial relation function).

Method	Interaction with Relative Spatial Information					Top-1 acc (%)
	Spatial Focus	(Quasi-)Global	Unique per Head	Nonlinear	Ordered	
Local SA	✓	-	-	-	-	81.0
RPC	✓	✓	✓	-	-	81.9
SP-SA Linear	✓	✓	✓	-	✓	82.2
SP-SA	✓	✓	✓	✓	✓	83.6

scores. To validate the effectiveness of our method, we compare it to several existing SA variants that also consider relative spatial information. As shown in Tab. 4, our SP-SA has much higher Top-1 accuracy, compared to SA with 1D RPE and 2D RPE. Most importantly, relative Positional Embeddings do not impose any beneficial inductive bias to the vanilla SA as our SP. Further, its linear form is not capable of capturing sophisticated 2D spatial relations. In addition, the value of $\vec{x}W^Q$ in Eq. (9) changes dynamically for every different input query. If an appropriate interaction between the content query and the positional embedding is always supposed to be achieved, a sufficiently large capacity is indispensable. However, this is not the case for the simple multiplication of query and relative positional embedding.

4.2.5 Comparing to Relative Positional Bias. As opposed to our method, the Relative Positional Bias [15] directly adds a univariate bias term to the content score between query-key pairs before applying softmax, and the bias term is taken from a learnable parameter table based on the relative coordinates. Adding such a bias term is a straightforward idea to include relative spatial information, but it is neither based on the idea of nor capable of learning complex abstracted 2D spatial priors, as reflected in the results in Tab. 4.

4.2.6 Comparing to Positional Self-Attention. To compare our proposed learnable spatial relation function with the hand-crafted Positional Self-Attention [5] in Eq. (8), we have also compared SP-SA to Positional Self-Attention in Tab. 4. Our method delivers better performance in this case of training a small model on limited data. This shows that the effort in such a manual design process can be saved by our learnable SP.

4.2.7 Importance of the Spatial Relation Function. To further validate the importance of our proposed spatial relation function, we compare it to different ways of multiplicative interaction with relative spatial information in Tab. 5. SP-SA Linear is obtained by removing the Relu of the default 2-layer Multi-Layer-Perceptron (MLP), and RPC is constructed by replacing our spatial relation function directly with coefficients taken from a parameter table, analogous to Relative Positional Bias [15]. For Local SA, we calculate attention scores only within a 7x7 local window. This is simply approximated by adopting Eq. (7) with $a = b = 1/3$ and $\vec{\Delta} = (0, 0)$. The results in Tab. 5 indicate that powerful non-linear functions are necessary to learn effective spatial priors.

Table 6: The effect of unique Spatial Priors (SPs) per head. This setting performs better than unique SPs per layer as well as shared SPs.

SP-SA	Top-1 (%)
shared SP	82.6
unique SPs per layer	82.1
unique SPs per layer&head (default)	83.6

4.2.8 Single vs Multiple Spatial Priors. To validate the benefit of combining various SPs, we compare our SP-SA to two of its variants: one only adopting a single SP for each layer, the other learning the same SP for the whole network. The results are reported in Tab. 6. A shared SP for the whole network thereby provides better results than learning a single SP for each layer. However, the proposed setting with a unique learnable SP per layer&head performs best, providing evidence of the benefit of combining different SPs.

5 CONCLUSIONS AND DISCUSSIONS

In this paper, we introduce a variant of Vanilla self-attention (SA) named Spatial Prior-enhanced Self-Attention (SP-SA) to facilitate vision transformers with automatically learned spatial priors. Based on the SP-SA, we further proposed SP-ViT and experimentally demonstrate the effectiveness of our method. Our proposed SP-ViTs of different sizes all establish state-of-the-art results for models trained on ImageNet-1K only. For example, SP-ViT-M achieves a 0.8% higher accuracy comparing to the previous state-of-the-art LV-ViT-M. We hope that our powerful SP-SA can stimulate more studies on designing and utilizing appropriate inductive biases for vision transformers. Finally, the learned spatial priors can be binarized and used for designing more computation-efficient transformers.

Limitations In spite of the excellent performance, vision transformers rely on heavy data augmentation techniques and the attention mechanism is computationally inefficient in comparison to convolution. Further investigations on improving ViTs are still desired.

REFERENCES

- [1] Tom B. Brown, Benjamin Mann, Nick Ryder, Melanie Subbiah, Jared Kaplan, Prafulla Dhariwal, Arvind Neelakantan, Pranav Shyam, Girish Sastry, Amanda Askell, Sandhini Agarwal, Ariel Herbert-Voss, Gretchen Krueger, Tom Henighan, Rewon Child, Aditya Ramesh, Daniel M. Ziegler, Jeffrey Wu, Clemens Winter, Christopher Hesse, Mark Chen, Eric Sigler, Mateusz Litwin, Scott Gray, Benjamin Chess, Jack Clark, Christopher Berner, Sam McCandlish, Alec Radford, Ilya Sutskever, and Dario Amodei. 2020. Language Models are Few-Shot Learners. In *Advances in Neural Information Processing Systems*, Vol. 33. 1877–1901.
- [2] Hila Chefer, Shir Gur, and Lior Wolf. 2021. Transformer Interpretability Beyond Attention Visualization. In *Proceedings of the IEEE/CVF Conference on Computer Vision and Pattern Recognition (CVPR)*. 782–791.
- [3] Chun-Fu Chen, Quanfu Fan, and Rameswar Panda. 2021. CrossViT: Cross-Attention Multi-Scale Vision Transformer for Image Classification. In *Proceedings of the IEEE/CVF International Conference on Computer Vision*. 357–366.
- [4] Zihang Dai, Hanxiao Liu, Quoc V. Le, and Mingxing Tan. 2021. CoAtNet: Marrying Convolution and Attention for All Data Sizes. *arXiv preprint arXiv:2106.04803* (2021).
- [5] Stéphane d’Ascoli, Hugo Touvron, Matthew Leavitt, Ari Morcos, Giulio Biroli, and Levent Sagun. 2021. ConViT: Improving Vision Transformers with Soft Convolutional Inductive Biases. In *ICML 2021: 38th International Conference on Machine Learning*.
- [6] Jacob Devlin, Ming-Wei Chang, Kenton Lee, and Kristina N. Toutanova. 2018. BERT: Pre-training of Deep Bidirectional Transformers for Language Understanding. In *Proceedings of the 2019 Conference of the North American Chapter of the Association for Computational Linguistics: Human Language Technologies, Volume 1 (Long and Short Papers)*. 4171–4186.
- [7] Xiaoyi Dong, Jianmin Bao, Dongdong Chen, Weiming Zhang, Nenghai Yu, Lu Yuan, Dong Chen, and Baining Guo. 2021. CSWin Transformer: A General Vision Transformer Backbone with Cross-Shaped Windows. *arXiv preprint arXiv:2107.00652* (2021).
- [8] Alexey Dosovitskiy, Lucas Beyer, Alexander Kolesnikov, Dirk Weissenborn, Xiaohua Zhai, Thomas Unterthiner, Mostafa Dehghani, Matthias Minderer, Georg Heigold, Sylvain Gelly, Jakob Uszkoreit, and Neil Houlsby. 2021. An Image is Worth 16x16 Words: Transformers for Image Recognition at Scale. In *ICLR 2021: The Ninth International Conference on Learning Representations*.
- [9] Chengyue Gong, Dilin Wang, Meng Li, Vikas Chandra, and Qiang Liu. 2021. Improve Vision Transformers Training by Suppressing Over-smoothing. *arXiv: Computer Vision and Pattern Recognition* (2021).
- [10] Benjamin Graham, Alaaeldin El-Nouby, Hugo Touvron, Pierre Stock, Armand Joulin, Hervé Jégou, and Matthijs Douze. 2021. LeViT: a Vision Transformer in ConvNet’s Clothing for Faster Inference. *arXiv preprint arXiv:2104.01136* (2021).
- [11] Kai Han, An Xiao, Enhua Wu, Jianyuan Guo, Chunjing Xu, and Yunhe Wang. 2021. Transformer in Transformer. *arXiv preprint arXiv:2103.00112* (2021).
- [12] Pengcheng He, Xiaodong Liu, Jianfeng Gao, and Weizhu Chen. 2021. DEBERTA: DECODING-ENHANCED BERT WITH DISENTANGLED ATTENTION. In *ICLR 2021: The Ninth International Conference on Learning Representations*.
- [13] Zihang Jiang, Qibin Hou, Li Yuan, Daquan Zhou, Yujun Shi, Xiaojie Jin, Anran Wang, and Jiashi Feng. 2021. All Tokens Matter: Token Labeling for Training Better Vision Transformers. *arXiv preprint arXiv:2104.10858* (2021).
- [14] Yinhan Liu, Myle Ott, Naman Goyal, Jingfei Du, Mandar Joshi, Danqi Chen, Omer Levy, Mike Lewis, Luke Zettlemoyer, and Veselin Stoyanov. 2019. RoBERTa: A Robustly Optimized BERT Pretraining Approach. *arXiv preprint arXiv:1907.11692* (2019).
- [15] Ze Liu, Yutong Lin, Yue Cao, Han Hu, Yixuan Wei, Zheng Zhang, Stephen Lin, and Baining Guo. 2021. Swin Transformer: Hierarchical Vision Transformer Using Shifted Windows. In *Proceedings of the IEEE/CVF International Conference on Computer Vision*. 10012–10022.
- [16] Zhuang Liu, Hanzi Mao, Chao-Yuan Wu, Christoph Feichtenhofer, Trevor Darrell, and Saining Xie. 2022. A ConvNet for the 2020s. *arXiv preprint arXiv:2201.03545* (2022).
- [17] Adam Paszke, Sam Gross, Francisco Massa, Adam Lerer, James Bradbury, Gregory Chanan, Trevor Killeen, Zeming Lin, Natalia Gimelshein, Luca Antiga, Alban Desmaison, Andreas Kopf, Edward Yang, Zachary DeVito, Martin Raison, Alykhan Tejani, Sasank Chilamkurthy, Benoit Steiner, Lu Fang, Junjie Bai, and Soumith Chintala. 2019. PyTorch: An Imperative Style, High-Performance Deep Learning Library. In *Advances in Neural Information Processing Systems*, Vol. 32. 8026–8037.
- [18] Peter Shaw, Jakob Uszkoreit, and Ashish Vaswani. 2018. Self-Attention with Relative Position Representations. In *Proceedings of the 2018 Conference of the North American Chapter of the Association for Computational Linguistics: Human Language Technologies, Volume 2 (Short Papers)*, Vol. 2. 464–468.
- [19] Mingxing Tan and Quoc Le. 2019. EfficientNet: Rethinking model scaling for convolutional neural networks. In *International Conference on Machine Learning*. PMLR, 6105–6114.
- [20] Hugo Touvron, Matthieu Cord, Douze Matthijs, Francisco Massa, Alexandre Sablayrolles, and Herve Jegou. 2021. Training data-efficient image transformers & distillation through attention. In *ICML 2021: 38th International Conference on Machine Learning*.
- [21] Hugo Touvron, Matthieu Cord, Alexandre Sablayrolles, Gabriel Synnaeve, and Hervé Jégou. 2021. Going deeper with Image Transformers. In *Proceedings of the IEEE/CVF International Conference on Computer Vision*. 32–42.
- [22] Ashish Vaswani, Noam Shazeer, Niki Parmar, Jakob Uszkoreit, Llion Jones, Aidan N. Gomez, Lukasz Kaiser, and Illia Polosukhin. 2017. Attention is All you Need. In *Proceedings of the 31st International Conference on Neural Information Processing Systems*, Vol. 30. 5998–6008.
- [23] Wenhai Wang, Enze Xie, Xiang Li, Deng-Ping Fan, Kaitao Song, Ding Liang, Tong Lu, Ping Luo, and Ling Shao. 2021. Pyramid Vision Transformer: A Versatile Backbone for Dense Prediction without Convolutions. *arXiv preprint arXiv:2102.12122* (2021).
- [24] Haiping Wu, Bin Xiao, Noel Codella, Mengchen Liu, Xiyang Dai, Lu Yuan, and Lei Zhang. 2021. CvT: Introducing Convolutions to Vision Transformers. *arXiv preprint arXiv:2103.15808* (2021).
- [25] Zhilin Yang, Zihang Dai, Yiming Yang, Jaime G. Carbonell, Ruslan Salakhutdinov, and Quoc V. Le. 2019. XLNet: Generalized Autoregressive Pretraining for Language Understanding. In *Advances in Neural Information Processing Systems*, Vol. 32. 5753–5763.
- [26] Kun Yuan, Shaopeng Guo, Ziwei Liu, Aojun Zhou, Fengwei Yu, and Wei Wu. 2021. Incorporating Convolution Designs into Visual Transformers. *arXiv preprint arXiv:2103.11816* (2021).
- [27] Li Yuan, Yunpeng Chen, Tao Wang, Weihao Yu, Yujun Shi, Francis E. H. Tay, Jiashi Feng, and Shuicheng Yan. 2021. Tokens-to-Token ViT: Training Vision Transformers from Scratch on ImageNet. *arXiv preprint arXiv:2101.11986* (2021).
- [28] Zizhao Zhang, Han Zhang, Long Zhao, Ting Chen, and Tomas Pfister. 2021. Aggregating Nested Transformers. *arXiv preprint arXiv:2105.12723* (2021).
- [29] Daquan Zhou, Bingyi Kang, Xiaojie Jin, Linjie Yang, Xiaochen Lian, Qibin Hou, and Jiashi Feng. 2021. DeepViT: Towards Deeper Vision Transformer. *arXiv preprint arXiv:2103.11886* (2021).